

# Inhomogeneously doped two-leg ladder systems

Stefan Wessel, Martin Indergand, Andreas Läuchli, Urs Ledermann, and Manfred Sigrist  
*Theoretische Physik, ETH-Hönggerberg, CH-8093 Zürich, Switzerland*  
(Dated: December 2, 2024)

A chemical potential difference between the legs of a two-leg ladder is found to be harmful for Cooper pairing. The instability of superconductivity in such systems is analyzed by comparing results of various analytical and numerical methods. Within a strong coupling approach for the  $t$ - $J$  model, supplemented by exact numerical diagonalization, hole binding is found unstable beyond a finite, critical chemical potential difference. The doping dependent phase diagram of the  $t$ - $J$  model, obtained from spinon-holon mean field theory, indicates a stepwise reduction of superconductivity upon increasing the chemical potential difference. Based on a renormalization group approach and Abelian bosonization, similar conclusions are reached for the weakly interacting Hubbard model.

## I. INTRODUCTION

Doped spin liquids have been an important subject of condensed matter research for the last two decades, mainly due to their possible relevance to the (cuprate) high-temperature superconductors (HTSCs).<sup>1,2</sup> Although it is still not understood how high-temperature superconductivity emerges from an antiferromagnetic Mott-insulator upon carrier doping, there is broad consensus that an intermediate pseudogap phase plays a crucial role in understanding both the exotic normal and superconducting properties of these materials.<sup>3</sup>

Many proposals concerning the nature of the pseudogap phase have emerged. One candidate for the pseudogap phase is the resonating valence bond state (RVB), which describes strongly fluctuating short-ranged spin singlets.<sup>1</sup> While the relevance of this state to the quasi-two-dimensional HTSCs is still under debate, it is realized in specially designed lattice structures.<sup>4</sup> Of particular interest are systems with ladder-shaped crystal structures, which are realized in various transition metal oxide compounds.<sup>5,6</sup>

Undoped, these ladder-systems are Mott-insulators and well described by quantum spin-1/2 Heisenberg models. For the two-leg ladder the ground state is an RVB-like state displaying short-ranged spin-singlet correlations with spin-singlet dimers on the rungs dominating over those along the legs. This constitutes a spin liquid with a finite energy gap to the lowest spin excitations. Furthermore, it was proposed that such a system would exhibit superconductivity upon hole-doping.<sup>7,8</sup> Various theoretical approaches confirmed a strong tendency towards formation of Cooper pairs with phase properties reminding of the  $d_{x^2-y^2}$ -wave channel of the two-dimensional HTSCs.<sup>9,10,11</sup>

The theoretical proposals were followed by an intense material research attempting to dope holes into a variety of known insulating copper-oxide compounds displaying ladder structures.<sup>12</sup> Materials under consideration are  $\text{SrCu}_2\text{O}_3$ ,  $\text{CaCu}_2\text{O}_3$ ,  $\text{LaCuO}_{2.5}$ , and  $\text{Sr}_{14}\text{Cu}_{24}\text{O}_{41}$ . Doping these compounds is intrinsically difficult because of chemical instabilities, and carrier localization effects may inhibit the desired metallic behavior. Nevertheless, the

search for superconductivity has been successful in the compound  $\text{Sr}_{14-x}\text{Ca}_x\text{Cu}_{24}\text{O}_{41}$  which contains layers of ladders alternating with layers of single chains.<sup>13</sup> In this material  $T_c$  rises up to about 12 K under high pressure, which apparently leads to a transfer of charge carriers from the chains onto the ladders. However, a detailed understanding of this system under high pressure has not been reached yet. A well-controlled and less invasive way of doping a ladder compound is thus highly desirable.

Recently, hole and electron doping of semiconductors and insulators by means of field effect devices has been proposed.<sup>14</sup> Here, mobile charge carriers are induced into the originally insulating material using a large gate voltage. This method would be ideal for doping quasi one- and two-dimensional systems, since the induced charge is confined to the outer-most layer of the compound, closest to the gate. Using this technique, success in doping the ladder compound  $\text{CaCu}_2\text{O}_3$  was reported, and superconductivity with a maximal  $T_c$  of 14 K was observed at atmospheric pressure.<sup>15</sup> An alternative technique of tunable doping has been achieved using heterostructures of layered materials such high- $T_c$  cuprates combined with ferroelectrics like  $\text{Pb}(\text{Zr},\text{Ti})\text{O}_3$ <sup>16,17,18</sup>. These non-volatile techniques of tunable doping may allow for a detailed comparison between experiment and theory in these low-dimensional structures.

The most natural choice of a ladder system for this type of doping control is a film in which the ladder planes lie parallel to the gate or ferroelectric, so that the carriers enter the ladders uniformly. This is the case for  $\text{CaCu}_2\text{O}_3$  and would be the same, in principle, for  $\text{SrCu}_2\text{O}_3$ . On the other hand, in the compound  $\text{LaCuO}_{2.5}$  the ladders are not parallel to each other, but exhibit a staggering.<sup>19</sup> Consequently, in a field effect device the ladders would be inhomogeneously doped in the sense that the chemical potential on the two legs would be different. Similarly, a variable orientation of the dipolar moments of the ferroelectric can lead to inhomogeneous doping.

In this paper we analyze the evolution of the superconducting state under such doping circumstances. Our analytical and numerical analysis shows that non-uniform doping is harmful to the superconducting state of the two-leg ladder. We derive phase diagrams for the strongly interacting  $t$ - $J$  model and the weakly interact-

ing Hubbard model in terms of the doping concentration, and the difference in the chemical potential on the legs,  $\Delta\mu$ . While for small  $\Delta\mu$  the ladder remains superconducting, the pairing is suppressed upon increasing  $\Delta\mu$ , and depending on the doping level new phases with reduced, and eventually without superconductivity appear.

The paper is organized according to the used analytical and numerical methods. In this way we study various aspects of the problem within different approximative schemes. In the following section a qualitative argument for the limited stability of the superconducting state upon inhomogeneous doping is presented. In Sec. III, a discussion of numerical exact diagonalization results is given for the charge correlations of two holes in ladders with up to 22 sites. Then, in Sec. IV we consider a mean field treatment of the  $t$ - $J$  model based on the spinon-holon decoupling scheme. In Sec. V, we apply renormalization group (RG) and bosonization methods to derive the phase diagram of the weakly interacting Hubbard model in the inhomogeneously doped case. We conclude in Sec. VI and draw a unified picture of the behavior of inhomogeneously doped two-leg ladder systems by combining the results from the earlier sections.

## II. STRONG RUNG COUPLING LIMIT

The influence of a difference in the chemical potential on the pairing state of the two-leg ladder can be illustrated by a simple qualitative argument for the  $t$ - $J$  model. Consider the two-leg ladder with electrons moving along the legs and rungs with hopping matrix elements  $t$  and  $t'$  respectively, and nearest-neighbor spin exchange with exchange constants  $J$  and  $J'$ . The Hamiltonian of the  $t$ - $J$  model then reads

$$\begin{aligned} H = & -t \sum_{j,a,s} \mathcal{P}(c_{j,a,s}^\dagger c_{j+1,a,s} + \text{h.c.}) \mathcal{P} \\ & -t' \sum_{j,s} \mathcal{P}(c_{j,1,s}^\dagger c_{j,2,s} + \text{h.c.}) \mathcal{P} \\ & + J \sum_{j,a} (\mathbf{S}_{j,a} \cdot \mathbf{S}_{j+1,a} - \frac{1}{4} n_{j,a} n_{j+1,a}) \\ & + J' \sum_j (\mathbf{S}_{j,1} \cdot \mathbf{S}_{j,2} - \frac{1}{4} n_{j,1} n_{j,2}) \\ & - \sum_{j,a,s} \mu_a n_{j,a,s}. \end{aligned} \quad (1)$$

The operator  $c_{j,a,s}^\dagger$  ( $c_{j,a,s}$ ) creates (annihilates) an electron with spin  $s$  on site  $(j, a)$ , where  $j$  labels the rungs, and  $a = 1, 2$  the legs. The electron number operators are defined as  $n_{j,a,s} = c_{j,a,s}^\dagger c_{j,a,s}$ , and  $n_{j,a} = \sum_s n_{j,a,s}$ . The spin operators are

$$\mathbf{S}_{j,a}^\alpha = \frac{1}{2} \sum_{s,s'} c_{j,a,s}^\dagger \sigma_{ss'}^\alpha c_{j,a,s'}, \quad (2)$$

where  $\sigma^\alpha$ ,  $\alpha = 1, 2, 3$  are Pauli matrices. The constraint of excluded double occupancy is enforced by the projection operator

$$\mathcal{P} = \prod_{j,a} (1 - n_{j,a,\uparrow} n_{j,a,\downarrow}). \quad (3)$$

In the last line of Eq. (1) different chemical potentials on the two legs,  $\mu_a$ ,  $a = 1, 2$  describe an inhomogeneous doping of the system. Throughout this paper we assume  $\Delta\mu = \mu_1 - \mu_2 \geq 0$ , and refer to the leg with  $a = 1$  ( $a = 2$ ) as the upper (lower) leg. Furthermore, the overall doping concentration  $\delta = 1 - n$  fixes the average chemical potential  $\bar{\mu} = (\mu_1 + \mu_2)/2$ .

The phases of the  $t$ - $J$  model on the two-leg ladder for  $\Delta\mu = 0$  are well characterized.<sup>20</sup> At half-filling ( $\delta = 0$ ) with one electron per site the ladder is a (Mott-) insulating spin liquid. Upon removal of electrons, i.e. doping of holes, mobile carriers appear, resulting in a Luther-Emery liquid with gapless charge modes and gapped spin excitations. Furthermore, the gapless charge mode exhibits dominant superconducting correlations with d-wave-like phase structure.

We now discuss the effect of inhomogeneous doping on this superconducting state, described by  $\Delta\mu > 0$ . For many aspects of ladder systems the limit of strong rung-coupling gives useful insights into their basic properties. Therefore we first consider the Hamiltonian (1) in the limit  $J', t' \gg J, t$ . Neglecting the coupling along the legs entirely, the undoped system corresponds to a chain of decoupled rungs, and the groundstate becomes a product state of dimer spin-singlets on the rungs. Furthermore, the lowest spin excitation corresponds to exciting one rung-singlet to a triplet, at an energy expense of  $J'$ . The superconducting state, i.e. Cooper pairing, in the doped spin liquid is inferred from the fact that two doped holes rather reside on a single rung rather than to separate onto two rungs. This is the case if the dominant energy scale is the spin exchange interaction,  $J'$ . Then the cost of breaking two spin singlets is larger than the gain of kinetic energy from separating the two holes. Namely, for two holes on a single rung the energy is

$$E_{2h} = J' - 2\bar{\mu}, \quad (4)$$

while for a single hole

$$E_{1h} = J' - \bar{\mu} - \frac{1}{2} \sqrt{4(t')^2 + \Delta\mu^2}. \quad (5)$$

Pairing on a rung is favored, if

$$2E_{1h} - E_{2h} = J' - \sqrt{4(t')^2 + \Delta\mu^2} > 0, \quad (6)$$

which in the uniformly doped case ( $\Delta\mu = 0$ ) leads to the condition  $J' > 2t'$  for pairing. Obviously, a finite value of  $\Delta\mu$  weakens the pairing by reducing the above energy gain.

This simple observation of depairing under non-uniform doping is confirmed by more sophisticated approaches, as those considered in the following sections.

### III. EXACT DIAGONALIZATION

To extend the discussion of the two-hole problem beyond the strong coupling limit we performed exact diagonalizations of finite systems, using the Lanczos algorithm.<sup>21</sup> We considered the Hamiltonian (1) at isotropic coupling ( $t = t'$ ,  $J = J'$ ), and studied the half-filled system doped with two holes, using periodic boundary conditions. We studied systems of different length,  $L$ , containing 8 to 11 rungs, and furthermore considered different values of  $J/t$ .

Consistent with the strong coupling argument of Sec. II, the hole bound state is found to be unstable beyond a critical value of  $\Delta\mu > \Delta\mu_c$ . Furthermore for the range of parameters considered here ( $0.4 \leq J/t \leq 0.8$ ), this critical value is  $\Delta\mu_c \approx J'$ . This indicates that the physics of the system is quite well captured by the strong rung-coupling limit, with  $J'$  being the dominant energy scale for pairing.

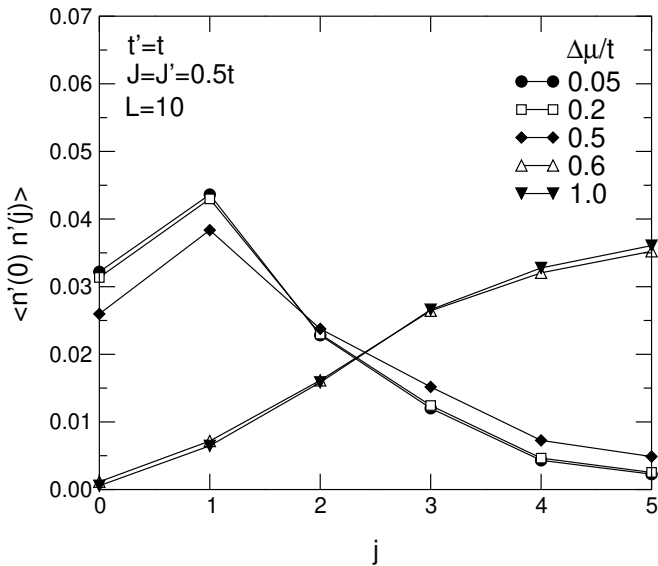


FIG. 1: Rung hole-hole correlation-function,  $\langle n'(0)n'(j) \rangle$ , in the ground state of the  $t\text{-}J$  model for an inhomogeneously doped two-leg ladder at selected values of the chemical potential difference,  $\Delta\mu$ . The finite ladder has  $L = 10$  rungs, and furthermore  $t = t'$ , and  $J = J' = 0.5t$ .

The behavior of the holes under non-uniform doping can be analysed using the hole-hole correlation function. Denoting the hole number operator on rung  $j$  by  $n'(j) = 2 - n_{j,1} - n_{j,2}$ , the rung hole-hole correlation function is defined as the ground state expectation value  $\langle n'(0)n'(j) \rangle$ , for the rung-rung separation  $j = 0, 1, \dots, \lfloor \frac{L}{2} \rfloor$ . This correlation function is shown in Fig. 1 for a ladder with 10 rungs for  $J/t = 0.5$ , and at selected values of the chemical potential difference,  $\Delta\mu$ . The behavior of the correlation function changes abruptly between  $\Delta\mu/t = 0.5$  and  $\Delta\mu/t = 0.6$ . For small values of  $\Delta\mu/t \leq 0.5$ , we find maximal rung hole-hole correlations between neighboring rungs, and a strong decay

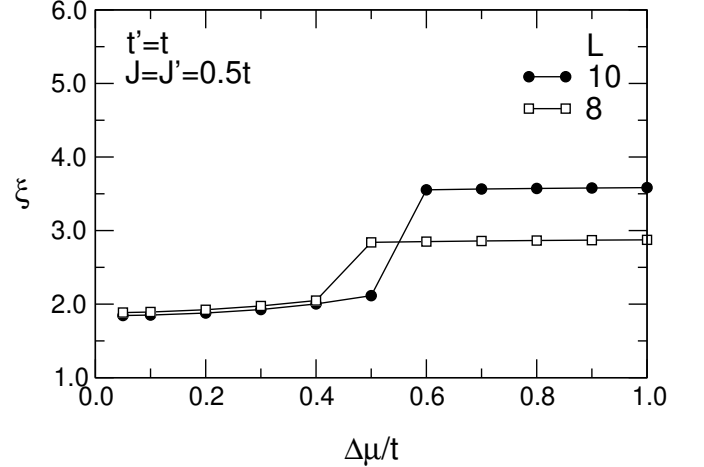


FIG. 2: Characteristic hole-hole separation length,  $\xi$ , in the ground state of the  $t\text{-}J$  model for an inhomogeneously doped two-leg ladder as a function of the difference in the chemical potential,  $\Delta\mu$ , for  $L = 8$  (squares), and  $L = 10$  (circles). Furthermore,  $t' = t$ , and  $J = J' = 0.5t$ .

of the correlation function at larger distances. For values of  $\Delta\mu/t \geq 0.6$ , the value of the correlation function is increasing with distance, and has a maximum value at the maximal possible rung-rung separation. Furthermore, it almost vanishes on the same rung. This clearly indicates the destruction of the hole-hole bound state for  $\Delta\mu/t \geq 0.6$ , where the system consists of two holes on the lower leg, favored by a lower chemical potential. The sudden change in the behavior of the correlation function is due to a level crossing at  $\Delta\mu_c$  in this system. While in the bound regime the ground state has zero total momentum along the legs, the lowest energy state in the unbound regime has a finite value of the total momentum. The correlation functions for  $\Delta\mu/t = 0.2$  and  $\Delta\mu/t = 0.05$  are almost identical, reflecting the robustness of the bound state against small doping inhomogeneities. Indeed, it can be shown that the doping asymmetry  $\Delta\mu$  does not have any effect in first order perturbation theory. In the regime of unbound holes the correlation function is again insensitive to changes in  $\Delta\mu$ , since for large  $\Delta\mu$  the holes are almost exclusively located on the lower leg, and therefore increasing  $\Delta\mu$  merely results in an overall energy shift.

The drastic change in the hole-hole correlation function as a result of the transition between the bound and unbound regime is also reflected in the characteristic hole-hole separation length,  $\xi$ , defined by

$$\xi^2 = \frac{1}{N} \sum_{j=-\lfloor \frac{L}{2} \rfloor}^{\lfloor \frac{L}{2} \rfloor - 1} j^2 \langle n'(0)n'(j) \rangle, \quad (7)$$

where  $N$  is a normalization factor given by  $N = \sum_j \langle n'(0)n'(j) \rangle$ . In Fig. 2, this separation length is plotted as a function of  $\Delta\mu$  for two different systems with an even number of rungs,  $L = 8$  and  $L = 10$ .<sup>22</sup> For both sys-

tems the characteristic hole-hole separation length jumps discontinuously at a critical value of  $\Delta\mu_c \approx J'$ . Furthermore, in the bound regime, i.e. for  $\Delta\mu \leq \Delta\mu_c$ , finite size effects in this quantity are rather small already for the system sizes considered here. In this regime the holes are bound, and the rung hole-hole correlation decays exponentially. Therefore, the bound pair wave function extends over only a few rungs. In the unbound regime however, the two holes tend to separate onto the lower leg, and therefore  $\xi$  grows with increasing system size.

The above numerical analysis demonstrates that non-uniform doping, by confining the mobile carriers onto one of the legs, is harmful to pairing. Furthermore, the inter-leg exchange interaction plays the important role of stabilizing the bound hole pair state. While the finite ladders considered in this section may be viewed as systems with a doping concentration of roughly  $\delta \sim 0.1$ , different approaches are needed to analyze the finite-doping regime beyond the two-hole problem. These will be presented in the following sections.

#### IV. MEAN FIELD ANALYSIS

In this section we extend our analysis of the  $t$ - $J$ -model by considering a mean field approximation based on the spinon-holon-decoupling scheme. We follow a similar approach as various previous studies on ladders as well as two-dimensional systems.<sup>20,23,24</sup>

##### A. Spinon-Holon Decomposition

The nonholonomic local constraint  $\sum_s c_{j,a,s}^\dagger c_{j,a,s} \leq 1$  is one of the main difficulties in treating the  $t$ - $J$ -model. The slave-boson formalism provides a possibility to take this constraint into account in an approximative way. Introducing fermionic spinon operators  $f$  and bosonic holon operators  $b$ , the electron creation and annihilation operators can be expressed as

$$c_{j,a,s}^\dagger = f_{j,a,s}^\dagger b_{j,a}, \quad \text{and} \quad c_{j,a,s} = b_{j,a}^\dagger f_{j,a,s}, \quad (8)$$

leading to the holonomic constraint

$$\sum_s f_{j,a,s}^\dagger f_{j,a,s} + b_{j,a}^\dagger b_{j,a} = 1. \quad (9)$$

The Hamiltonian (1) can be expressed in terms of this new operators as

$$\begin{aligned} H = & -t \sum_{j,a,s} (f_{j,a,s}^\dagger f_{j+1,a,s} b_{j,a} b_{j+1,a}^\dagger + \text{h.c.}) \\ & -t' \sum_{j,s} (f_{j,1,s}^\dagger f_{j,2,s} b_{j,1} b_{j,2}^\dagger + \text{h.c.}) \\ & + J \sum_{j,a,s} \mathbf{S}_{j,a}^f \cdot \mathbf{S}_{j+1,a}^f \\ & + J' \sum_{j,s} \mathbf{S}_{j,1}^f \cdot \mathbf{S}_{j,2}^f \\ & - \sum_{j,a} \lambda_a \left( \sum_s f_{j,a,s}^\dagger f_{j,a,s} + b_{j,a}^\dagger b_{j,a} - 1 \right) \\ & + \sum_{j,a} \mu_a b_{j,a}^\dagger b_{j,a}, \end{aligned} \quad (10)$$

where the Lagrange multipliers  $\lambda_a$ ,  $a = 1, 2$  have been introduced to enforce the local constraint (9) on average for each leg. In the exchange part, terms proportional to  $n_{j,a} n_{j',a'}$  have been neglected since in mean field approximations they tend to artificially enhance the tendency towards pairing.<sup>24</sup> Furthermore, the  $\mathbf{S}_{j,a}^f$  are defined in terms of spinon operators, and in all four-fermion terms the approximation  $b_{j,a} b_{j,a}^\dagger b_{j',a'} b_{j',a'}^\dagger = 1$  has been used, which becomes exact at half-filling. The last term in Eq. (10) takes the different chemical potentials on the two legs into account.

To proceed we decouple the terms which are not single particle terms in the Hamiltonian (10) by introducing the following mean fields<sup>23</sup>

$$\begin{aligned} \chi_{j,a;j',a'} &= \frac{1}{2} \sum_{\sigma} \langle f_{j,a,\sigma}^\dagger f_{j',a',\sigma} \rangle, \\ B_{j,a;j',a'} &= \langle b_{j,a} b_{j',a'}^\dagger \rangle, \\ \Delta_{j,a;j',a'} &= \langle f_{j,a,\downarrow} f_{j',a',\uparrow} \rangle. \end{aligned} \quad (11)$$

In the following the mean fields along the legs are labeled with the indices 1 and 2, and the mean field on the rung with the index 3, e.g. for  $\chi$ :

$$\begin{aligned} \chi_a &= \frac{1}{2} \sum_{\sigma} \langle f_{j,a,\sigma}^\dagger f_{j+1,a,\sigma} \rangle \quad a = 1, 2 \quad (12) \\ \chi_3 &= \frac{1}{2} \sum_{\sigma} \langle f_{j,1,\sigma}^\dagger f_{j,2,\sigma} \rangle. \end{aligned}$$

This convention of labeling the bond  $(j, a; j', a')$  also applies to the mean fields  $B$ , and  $\Delta$ .

Introducing the Fourier transformed operators

$$\begin{aligned} f_{k,a,\sigma} &= \frac{1}{\sqrt{L}} \sum_j f_{j,a,\sigma} e^{ikr_j}, \\ b_{k,a} &= \frac{1}{\sqrt{L}} \sum_j b_{j,a} e^{ikr_j}, \end{aligned} \quad (13)$$

the mean field Hamiltonian reads

$$H_{MF} = \sum_k (H_k^b + H_k^f) + L \left[ \sum_a \left\{ \frac{3}{2} J (\Delta_a^2 + \chi_a^2) + 4t\chi_a B_a \right\} + \frac{3}{2} J' (\Delta_3^2 + \chi_3^2) + 4t'\chi_3 B_3 \right]. \quad (14)$$

The quadratic terms  $H_k^b$  and  $H_k^f$  are given by

$$H_k^b = \begin{pmatrix} b_{k,1}^\dagger \\ b_{k,2}^\dagger \end{pmatrix}^\top \begin{bmatrix} -4t\chi_1 \cos k - \lambda_1 + \mu_1 & -2t'\chi_3 \\ -2t'\chi_3 & -4t\chi_2 \cos k - \lambda_2 + \mu_2 \end{bmatrix} \begin{pmatrix} b_{k,1} \\ b_{k,2} \end{pmatrix},$$

$$H_k^f = \begin{pmatrix} f_{k,1,\uparrow}^\dagger \\ f_{k,2,\uparrow}^\dagger \\ f_{-k,1,\downarrow} \\ f_{-k,2,\downarrow} \end{pmatrix}^\top \begin{bmatrix} \hat{\xi}_k & \hat{\Delta}_k \\ \hat{\Delta}_k & -\hat{\xi}_k \end{bmatrix} \begin{pmatrix} f_{k,1,\uparrow} \\ f_{k,2,\uparrow} \\ f_{-k,1,\downarrow}^\dagger \\ f_{-k,2,\downarrow}^\dagger \end{pmatrix},$$

where  $\hat{\xi}_k$ , and  $\hat{\Delta}_k$  are the following  $2 \times 2$  matrices

$$\hat{\xi}_k = \begin{bmatrix} -\lambda_1 - (2tB_1 + \frac{3}{2}J\chi_1) \cos k & -t'B_3 - \frac{3}{4}J'\chi_3 \\ -t'B_3 - \frac{3}{4}J'\chi_3 & -\lambda_2 - (2tB_2 + \frac{3}{2}J\chi_2) \cos k \end{bmatrix}, \quad \hat{\Delta}_k = \begin{bmatrix} -\frac{3}{2}J\Delta_1 \cos k & -\frac{3}{4}J'\Delta_3 \\ -\frac{3}{4}J'\Delta_3 & -\frac{3}{2}J\Delta_2 \cos k \end{bmatrix}.$$

The mean fields are determined by self-consistently solving the single-particle problem of  $H_{MF}$  and calculating the corresponding expectation values according to Eqs. (11,12).

Diagonalization of the bosonic part of the Hamiltonian yields two holon bands. In the ground state of the system, the holons are assumed to Bose condense into their lowest energy state. Denoting the amplitudes of the lowest holon state on the two legs by  $A_a = \langle b_a \rangle = \langle b_a^\dagger \rangle$ , the bosonic bond mean fields become

$$\begin{aligned} B_a &= 2\delta A_a^2, & a &= 1, 2, \\ B_3 &= 2\delta A_1 A_2. \end{aligned} \quad (15)$$

The spinon part of the Hamiltonian can be diagonalized by a Bogoliubov transformation, from which the self-consistent equations for the mean fields  $\Delta$  and  $\chi$ , and the Lagrange multipliers  $\lambda$  are determined numerically. Furthermore we define the BCS order parameters  $\Delta'$ , as<sup>24</sup>

$$\begin{aligned} \Delta'_{j,a;j',a'} &:= \langle c_{j,a,\uparrow} c_{j',a',\downarrow} \rangle \\ &\approx \langle b_{j,a}^\dagger b_{j',a'}^\dagger \rangle \langle f_{j,a,\uparrow} f_{j',a',\downarrow} \rangle = B_{j,a;j',a'} \Delta_{j,a;j',a'} \end{aligned} \quad (16)$$

in terms of the holon and spinon mean fields. For the BCS order parameters we use the same bond labeling scheme as in Eq. (12).

## B. Results

Within the above mean field description we are able to analyze the behavior of the two-leg ladder for differ-

ent values of the doping concentration,  $\delta$ , and chemical potential difference,  $\Delta\mu$ . In particular, we are interested in the BCS order parameters as the indication for Cooper paring. In the following the parameters of the  $t$ - $J$  model are fixed to isotropic couplings with  $t' = t$ , and  $J' = J = 0.5t$ . Furthermore, we restrict ourselves to the low doping region  $\delta < 0.25$ , where the above spinon-holon decomposition is expected to be qualitatively reliable.<sup>24</sup>

For  $\Delta\mu = 0$  our calculations confirm the overall behavior obtained from similar mean field calculations using a Gutzwiller-type renormalization method.<sup>20</sup> In Fig. 3 (a,b) the BCS mean fields  $\Delta'$  of Eq. (16) are plotted as functions of the doping concentration. While at half-filling ( $\delta = 0$ ) the BCS order parameters vanish, they increase monotonically with hole doping away from half filling. Their values on the legs coincide, i.e.  $\Delta'_1 = \Delta'_2$ , whereas a phase shift of  $\pi$  exists relative to the rung order parameter  $\Delta'_3$ , in analogy to the d-wave pairing symmetry on the square lattice version of the doped  $t$ - $J$ -model.

In order to analyze the destructive influence of a chemical potential difference between the two legs on the Cooper pairing, we follow the behavior of the BCS mean fields  $\Delta'_{1,2,3}$  for finite  $\Delta\mu > 0$ .

At a value of  $\Delta\mu = t$ , for which the corresponding BCS mean fields are shown in Fig. 3 (c,d), the holes prefer to enter the lower leg. This naturally tends to enhance the BCS mean field on this leg compared to the upper leg. In Fig. 3 (c,d) this tendency is clearly visible in addition to an overall reduction of the pairing amplitude, in particular in the low-doping region. The  $\delta$ -dependence indicates a regime change around  $\delta = 0.1$  suggesting a critical doping  $\delta_c$  for the BCS mean fields. Furthermore,

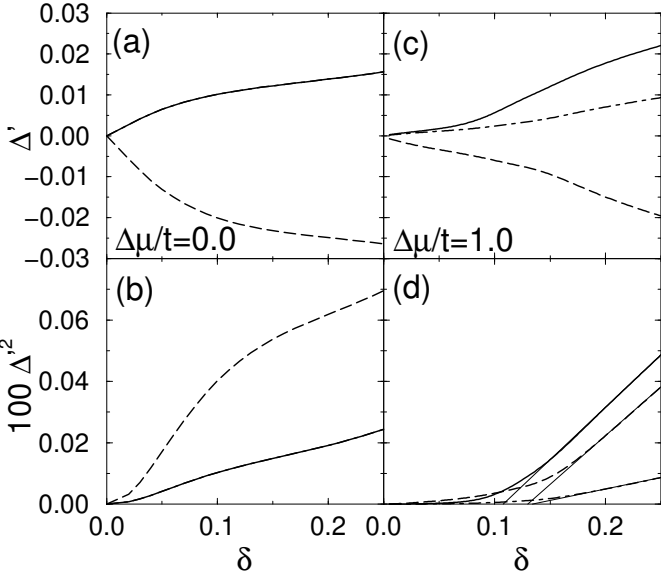


FIG. 3: BCS mean fields  $\Delta'$ (a,c) and  $\Delta'^2$ (b,d) of the  $t$ - $J$  model on a two-leg ladder as functions of the doping concentration,  $\delta$ , at constant  $\Delta\mu/t = 0.0$  (a,b) and  $\Delta\mu/t = 1.0$  (c,d), for  $t' = t$ , and  $J' = J = 0.5t$ . The mean fields on the lower (upper) leg are plotted with solid (dotted-dashed) lines, and those on the rungs using dashed lines. Straight lines in (d) extrapolate the linear behavior.

close to  $\delta_c$  the BCS mean fields vanish with an underlying  $\Delta' \propto \sqrt{\delta - \delta_c}$  dependence, as can most easily be observed for the squared values of the mean fields shown in Fig. 3 (d). The linear extrapolation yields the critical dopings  $\delta_c$ . Moreover, the destruction of superconductivity towards small doping progresses in steps. While the order parameter on the upper leg and the rungs disappear at the same doping concentration  $\delta_{c1} \approx 0.13$ , for the lower leg the critical doping is  $\delta_{c2} \approx 0.11$ . This behavior indicates that for small doping the ladder structure plays a reduced role as the few holes tend to be mainly confined onto the lower leg. The hole density on the upper leg is strongly reduced and results from virtual hopping processes. Only upon doping beyond  $\delta_{c1}$  the holes enter also the upper leg, enhancing the tendency to form pairs so that eventually the BCS mean fields grow rapidly. The absence of a sharp transition is an artifact of the spinon-holon mean field decoupling scheme.

Scanning the doping concentration,  $\delta$ , and the chemical potential difference,  $\Delta\mu$ , the phase diagram of Fig. 4 is obtained, based on the critical doping levels  $\delta_{c1,2}$  defined above. For small values of  $\Delta\mu$  the BCS order parameter with d-wave-like phase structure is realized, with both legs of the ladder involved in the paring state. Upon increasing  $\Delta\mu$  we turn into a different superconducting regime, where the BCS order parameter on the lower leg dominates the pairing, whereas the upper leg and the rungs participate only via a proximity effect.<sup>25,26</sup> Eventually, at high enough values of  $\Delta\mu$ , superconductivity completely disappears. For a doping  $\delta \sim 0.1$  this critical value of  $\Delta\mu$  is around  $0.75t$ , which compares well

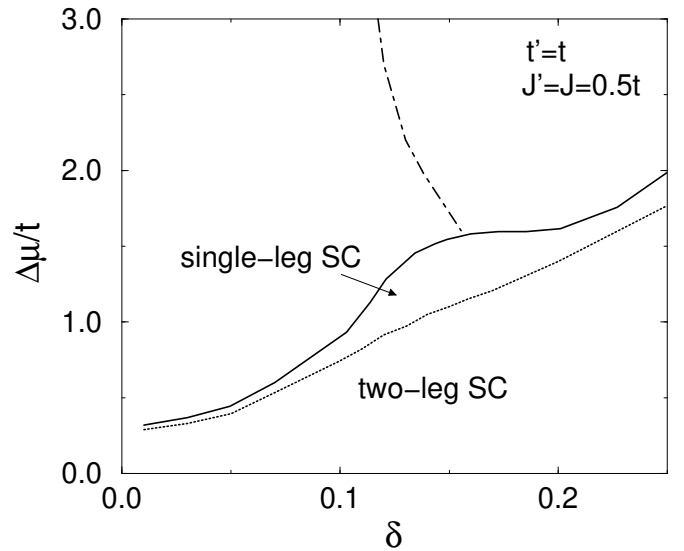


FIG. 4: Low doping phase diagram of the inhomogeneously doped two-leg ladder in the mean field approximation of the  $t$ - $J$  model at  $t' = t$ ,  $J' = J = 0.5t$ . The dotted line indicates the crossover between the two-leg and single-leg superconducting (SC) phases, while the solid line denotes the phase boundary to the normal phase. The dotted-dashed line separates a low-doping normal phase dominated by gapped spinon excitations from the higher-doping phase dominated by gapless spinon excitations.

with the value obtained from exact diagonalization (c.f. Sec. II).

In the large- $\Delta\mu$  region the mean field solution exhibits two distinct phases. To characterize these regions we study the behavior of the various mean fields along lines of constant doping, as shown for the BCS order parameters in Fig. 5. For a doping  $\delta = 0.1$ , shown in Fig. 5 (a,b), the pairing mean fields retain a finite tail up to large values of  $\Delta\mu$ , well beyond the apparent upper critical value of  $\Delta\mu_c/t \approx 0.9$  estimated by linear extrapolation (Fig. 5 (b)). This behavior is significantly different from the behavior for  $\delta = 0.2$  shown in Fig. 5 (c,d). In this case the mean fields vanish rather abruptly at a upper critical value of  $\Delta\mu_c/t \approx 1.6$ , obtained from Fig. 5(d).

The extended finite tails of the BCS mean fields at  $\delta = 0.1$  for  $\Delta\mu > \Delta\mu_c$  exhibit the presence of a spin excitation gap, i.e. despite pair breaking the mean field spinon spectrum obtained from Eq. (14) remains gapped. Thus the spin liquid state still dominates the behavior of the system, as low-energy spin excitations do not appear in our mean field solution. On the other hand, for  $\delta = 0.2$  the gap in the spinon excitation spectrum closes at the upper critical chemical potential difference,  $\Delta\mu_c$ . In general, the spin excitation spectrum is strongly renormalized by inter-spinon interactions from the spinon spectrum obtained from Eq. (14).<sup>20</sup> Nevertheless, the above analysis suggests that in the low doping regime the dominant spectral weight of the spin excitation spectrum is

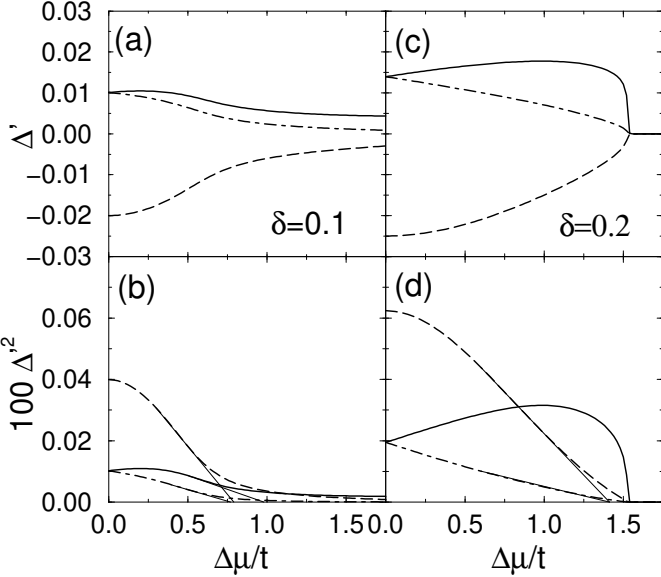


FIG. 5: BCS mean fields  $\Delta'$  (a,c) and  $\Delta'^2$  (b,d) of the  $t$ - $J$  model on a two-leg ladder as functions of the difference in the chemical potential,  $\Delta\mu$ , at constant doping  $\delta = 0.1$  (a,b), and  $\delta = 0.2$  (c,d), for  $t' = t$ ,  $J' = J = 0.5t$ . The fields on the lower (upper) leg are plotted using solid (dotted-dashed) lines, and those on the rung using dashed lines. Straight lines in (b,d) extrapolate the linear behavior.

located at finite energies. For larger values of the doping, however, decoupled spinon spectrums of a single spin chain and of a doped  $t$ - $J$  chain occur in the mean field solution. This corresponds to a phase separated state with different phases residing on the two legs, decoupled from each other. There is a clear phase boundary in our mean field calculation between these two regimes drawn by a dashed-dotted line in Fig. 4. However, there is no indication for a true phase transition, as the low-energy character of both phases is the same, namely that of a Luttinger liquid. Nevertheless, the slave-boson mean field theory emphasizes the dominant features, i.e. a RVB-like spin liquid at low doping, and a doped spin chain close to quarter filling.

The results obtained within slave-boson mean field theory clearly exhibit a limited stability of the superconducting phase upon inhomogeneously doping the two-leg ladder system. The conclusions obtained for the  $t$ - $J$  model are consistent with results from a renormalization group treatment of the Hubbard model, as presented in the following section.

## V. RENORMALIZATION GROUP

In order to complement the analysis of the  $t$ - $J$  model, in this section we consider the weakly interacting Hubbard model on a two-leg ladder. A renormalization group (RG) treatment supplemented by Abelian bosonization allows a detailed analysis of the phase diagram in the weakly interacting limit, and a characterization of the

various phases in terms of the low-energy modes. We follow an approach established on standard two- and N-leg ladder systems (i.e. for  $\Delta\mu = 0$ ).<sup>11,27,28,29</sup>

In the current case of an inhomogeneously doped two-leg ladder we consider the weak repulsive limit,  $0 < U \ll t, t'$  of the Hubbard model,

$$H = -t \sum_{j,a,s} (c_{j,a,s}^\dagger c_{j+1,a,s} + \text{h.c.}) - t' \sum_{j,s} (c_{j,1,s}^\dagger c_{j,2,s} + \text{h.c.}) + U \sum_{j,a} c_{j,a,\uparrow}^\dagger c_{j,a,\uparrow} c_{j,a,\downarrow}^\dagger c_{j,a,\downarrow} - \sum_{j,a,s} \mu_a c_{j,a,s}^\dagger c_{j,a,s}, \quad (17)$$

with the same notations as in Sec. I. The quadratic part of the Hamiltonian (17), i.e. Eq. (17) for  $U = 0$ , can be decoupled via a canonical transformation

$$d_{j,1/2,s}^\dagger = \sqrt{\frac{1 \mp \Delta\mu/D}{2}} c_{j,2,s}^\dagger \pm \sqrt{\frac{1 \pm \Delta\mu/D}{2}} c_{j,1,s}^\dagger, \quad (18)$$

where  $D = \sqrt{4t'^2 + \Delta\mu^2}$ . These rung operators interpolate smoothly between the bonding and anti-bonding combinations at  $\Delta\mu = 0$ , and the original fermions for  $\Delta\mu/t' \rightarrow \infty$ , where  $d_{j,i,s}^\dagger \rightarrow c_{j,i,s}^\dagger$ . In momentum space two bands corresponding to  $d_{i,s}^\dagger(k)$ ,  $i = 1, 2$  result with dispersions

$$\varepsilon_{1/2}(k) = -2t \cos(k) \pm \frac{1}{2}D - \bar{\mu}, \quad (19)$$

and a bandwidth  $4t$ .

Consider now the effect of the Hubbard interaction term in Eq. (17). When both bands are completely separated in energy, only the lower band is filled, and at half filling ( $\delta = 0$ ) a band insulator is obtained which upon doping ( $\delta > 0$ ) becomes an ordinary spin-1/2 Luttinger liquid (LL). For  $D < 4t \cos^2(\pi\delta)$ , both bands are partially filled, and inter-band interaction effects must be examined. While this proves difficult in general, progress can be made upon considering the weakly interacting limit. Since the interest is thus on the low-energy physics, the dispersions (19) can be linearized around the Fermi points  $k_{F,i}$ ,  $i = 1, 2$ , determined by  $\varepsilon_1(k_{F,1}) = \varepsilon_2(k_{F,2})$  and  $k_{F,1} + k_{F,2} = \pi(1 - \delta)$ . Furthermore left- and right movers,  $d_{R/L,i,s}^\dagger$ , are defined with respect to the Fermi level in each band,  $i = 1, 2$ . For generic (i.e. incommensurate) Fermi momenta the interactions consist of intra- and inter-band forward- and Cooper- scattering. These can be organized in terms of the  $U(1)$  and  $SU(2)$  current operators

$$J_{p,i,j} = \sum_s d_{p,i,s}^\dagger d_{p,j,s}, \quad J_{p,i,j}^\alpha = \frac{1}{2} \sum_{s,s'} d_{p,i,s}^\dagger \sigma_{s,s'}^\alpha d_{p,j,s'}, \quad (20)$$

where  $p = R, L$ , and the band indices  $i, j = 1, 2$ . The following non-chiral current-current interactions are allowed by symmetry,

$$\begin{aligned} H_I = & \sum_{i=1,2} \int dx (c_{ii}^\rho J_{R,i,i} J_{L,i,i} - c_{ii}^\sigma \mathbf{J}_{R,i,i} \cdot \mathbf{J}_{L,i,i}) \\ & + 2 \int dx (c_{12}^\rho J_{R,1,2} J_{L,1,2} - c_{12}^\sigma \mathbf{J}_{R,1,2} \cdot \mathbf{J}_{L,1,2}) \\ & + 2 \int dx (f_{12}^\rho J_{R,1,1} J_{L,2,2} - f_{12}^\sigma \mathbf{J}_{R,1,1} \cdot \mathbf{J}_{L,2,2}). \end{aligned} \quad (21)$$

In this representation  $f$  ( $c$ ) denotes couplings related to forward- (Cooper-) scattering, and the symmetry of the inter-band scattering terms under the band exchange is explicitly taken into account. Using current algebra and operator product expansions, a one-loop RG flow for the various couplings can be derived,<sup>11</sup> which in our notation reads

$$\begin{aligned} \frac{dc_{ii}^\rho}{dl} &= -\frac{1}{2v_i} \left[ (c_{ii}^\rho)^2 + \frac{3}{16} (c_{ii}^\sigma)^2 \right], \\ \frac{dc_{ii}^\sigma}{dl} &= -\frac{1}{2v_i} \left[ \frac{1}{2} (c_{ii}^\sigma)^2 + 2c_{ii}^\rho c_{ii}^\sigma \right] - \frac{1}{2v_i} (c_{ii}^\sigma)^2, \\ \frac{dc_{12}^\rho}{dl} &= -\sum_i \frac{1}{2v_i} \left[ c_{1i}^\rho c_{i2}^\rho + \frac{3}{16} c_{1i}^\sigma c_{i2}^\sigma \right] \\ &\quad + \frac{2}{v_1 + v_2} \left[ c_{12}^\rho f_{12}^\rho + \frac{3}{16} c_{12}^\sigma f_{12}^\sigma \right], \\ \frac{dc_{12}^\sigma}{dl} &= -\sum_i \frac{1}{2v_i} \left[ c_{1i}^\rho c_{i2}^\sigma + c_{1i}^\sigma c_{i2}^\rho + \frac{1}{2} c_{1i}^\sigma c_{i2}^\sigma \right] \quad (22) \\ &\quad + \frac{2}{v_1 + v_2} \left[ c_{12}^\rho f_{12}^\sigma + c_{12}^\sigma f_{12}^\rho - \frac{1}{2} c_{12}^\sigma f_{12}^\sigma \right], \\ \frac{df_{12}^\rho}{dl} &= \frac{1}{v_1 + v_2} \left[ (c_{12}^\rho)^2 + \frac{3}{16} (c_{12}^\sigma)^2 \right], \\ \frac{df_{12}^\sigma}{dl} &= \frac{1}{v_1 + v_2} \left[ 2c_{12}^\rho c_{12}^\sigma - \frac{1}{2} (c_{12}^\sigma)^2 - (f_{12}^\sigma)^2 \right], \end{aligned}$$

where  $i = 1, 2$ ,  $\bar{1} = 2$ ,  $\bar{2} = 1$ , and  $v_i = 2t \sin(k_{F,i})$  are the Fermi velocities for the bands. The successive elimination of high frequency modes is obtained from (22) by integration along the logarithmic length scale  $l$ , related to an energy scale  $E \sim te^{-\pi l}$ . The flow equations can be integrated once the bare values of the couplings are known. For the Hubbard interaction of Eq. (17) they are obtained as

$$\begin{aligned} c_{11}^\sigma &= c_{22}^\sigma = 4c_{11}^\rho = 4c_{22}^\rho = U \left[ 1 + \left( \frac{\Delta\mu}{D} \right)^2 \right], \\ c_{12}^\sigma &= 4c_{12}^\rho = f_{12}^\sigma = 4f_{12}^\rho = U \left[ 1 - \left( \frac{\Delta\mu}{D} \right)^2 \right]. \end{aligned} \quad (23)$$

Increasing  $\Delta\mu$  away from zero can be seen to reduce the bare inter-band scattering with respect to intra-band scattering.

Depending on the parameters, integration of the flow equations leads to different asymptotic behavior, with either a flow to a finite-valued fix point, or to instabilities characterized by universal ratios of the renormalized couplings beyond a scale  $l^*$ , where the most diverging coupling becomes of the order the bandwidth. While the consistency of the one-loop renormalization group equations is restricted to  $l < l^*$ , the asymptotic ratios can be utilized to derive a description of the low-energy physics of the system within Abelian bosonization.<sup>30</sup> Introducing canonically conjugated bosonic fields  $\Phi_{\nu i}$ , and  $\Pi_{\nu i}$  for the charge and spin degrees of freedom ( $\nu = \rho, \sigma$ ) on each band  $i = 1, 2$ , the fermionic operators can be represented as

$$d_{R/L,i,s} = \frac{\eta_{is}}{\sqrt{2\pi\alpha}} e^{i\sqrt{\pi/2}[\pm(\Phi_{\nu i} + s\Phi_{\sigma i}) - (\theta_{\nu i} + s\theta_{\sigma i})]}, \quad (24)$$

where  $\theta_{\nu i}$  is the dual field of  $\Phi_{\nu i}$ , so that  $\partial_x \theta_{\nu i} = \Pi_{\nu i}$ . The  $\eta_{is}$  are Klein factors, ensuring anticommutation relations, and  $\alpha$  is a short-distance cutoff.<sup>31</sup> Using the above representation, the interacting fermionic Hamiltonian transforms into a bosonic Hamiltonian,  $H_B = H_q + H_I$ , containing quadratic terms

$$\begin{aligned} H_q = & \sum_{\nu,i} \frac{1}{2} \int dx \left[ v_i + \frac{c_{ii}^\nu}{\beta_\nu |\beta_\nu|} \right] \partial_x \Phi_{\nu i}^2 + \left[ v_i - \frac{c_{ii}^\nu}{\beta_\nu |\beta_\nu|} \right] \Pi_{\nu i}^2 \\ & + \int dx \frac{f_{12}^\nu}{\beta_\nu |\beta_\nu|} (\partial_x \Phi_{\nu 1} \partial_x \Phi_{\nu 2} - \Pi_{\nu 1} \Pi_{\nu 2}), \end{aligned} \quad (25)$$

and sine-Gordon-like interaction terms

$$\begin{aligned} H_I = & \int dx \{ c_{11}^\sigma \cos(\sqrt{2}\beta_\sigma \Phi_{\sigma 1}) + c_{22}^\sigma \cos(\sqrt{2}\beta_\sigma \Phi_{\sigma 2}) \\ & - 4c_{12}^\rho \cos(2\beta_\rho \theta_{\rho -}) [\cos(\beta_\sigma \Phi_{\sigma -}) - \cos(\beta_\sigma \theta_{\sigma -})] \\ & - c_{12}^\sigma \cos(2\beta_\rho \theta_{\rho -}) [2\cos(\beta_\sigma \Phi_{\sigma +}) + \cos(\beta_\sigma \Phi_{\sigma -})] \\ & - c_{12}^\sigma \cos(2\beta_\rho \theta_{\rho -}) \cos(\beta\theta_{\sigma -}) \\ & + 2f_{12}^\sigma \cos(\beta_\sigma \theta_{\sigma -}) \cos(\beta_\sigma \Phi_{\sigma +}) \}, \end{aligned} \quad (26)$$

where  $\beta_\rho = \sqrt{\pi}$ ,  $\beta_\sigma = -\sqrt{4\pi}$ , and the fields  $\Phi_{\nu \pm} = (\Phi_{\nu 1} \pm \Phi_{\nu 2})/\sqrt{2}$  and  $\Pi_{\nu \pm} = (\Pi_{\nu 1} \pm \Pi_{\nu 2})/\sqrt{2}$  have been introduced. Upon minimizing the energy in a semiclassical approximation, any coupling that diverges under the RG flow opens up a gap for a field that is pinned by the corresponding terms in (26).

Performing the above procedure, four different phases are obtained for the Hamiltonian of Eq. (17), shown in the  $(\delta, \Delta\mu)$ -plane for isotropic hopping,  $t' = t$ , in Fig. 6. The various phases are labeled according to the number of gapless charge (n) and spin (m) modes by CnSm. The different asymptotic regimes of the RG flow (22) are related to the phases shown in Fig. 5 as follows:

(C1S1) The single band LL. This phase with an empty upper band is labeled C1S1, reflecting the number of gapless modes. For incommensurate filling the dominant correlations are charge density waves (CDW) and spin density waves (SDW).<sup>31</sup>

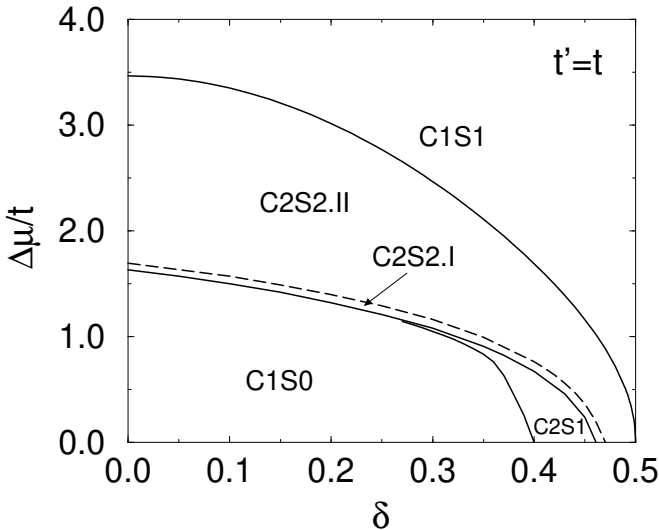


FIG. 6: Phase diagram of the inhomogeneously doped Hubbard model on two-leg ladder in the weakly interacting limit, and for  $t' = t$ . The phases  $C_nS_m$  are labeled according to the number of gapless charge ( $n$ ) and spin ( $m$ ) modes. Solid lines are phase boundaries. The dashed line indicates the crossover from a region with dominant SC correlations in the lower and CDW and SDW correlations in the upper band (C2S2.I), to a region dominated by CDW and SDW correlations in both bands, for larger values of  $\Delta\mu$  (C2S2.II).

(C2S2) The trivial fixed point. In this regime the couplings stay of order  $U$  under the RG flow, or renormalize to zero. Therefore no gap opens in this phase, labeled C2S2. Furthermore, the two partially filled bands are decoupled in this regime. Standard LL theory<sup>31</sup>, used to determine the dominant correlations within each band, indicates a crossover between two regions labeled C2S2.I, and C2S2.II respectively, c.f. Fig. 6. The dominant correlations in the C2S2.II regime are CDW and SDW within both bands, whereas in the C2S2.I regime the lower band is dominated by superconducting (SC) fluctuations.

(C2S1) Single-band superconductivity. Here, all couplings stay of the order of  $U$  or renormalize to zero, except for  $c_{22}^\sigma \sim -v_2$ . This results in a pinning of the spin mode of the lower band, and the number of gapless modes reduces to C2S1. SC correlations dominate the lower band, and CDW and SDW correlations the upper band. Furthermore, inter-band phase coherence is not established within this regime.

(C1S0) Inter-band superconductivity. In this regime the diverging couplings flow towards the asymptotic ratios

$$4c_{12}^\rho = 8f_{12}^\rho = c_{12}^\sigma, \quad c_{11}^\sigma/v_1 = c_{22}^\sigma/v_2. \quad (27)$$

From the low-energy effective bosonic Hamiltonian two finite spin gaps are obtained, and a pinning of the charge mode  $\theta_{\rho-} = 0$ , resulting in phase coherence between the

two bands. The number of gapless modes is reduced to C1S0. The remaining total charge mode,  $(\Phi_{\rho+}, \theta_{\rho+})$ , is gapless and exhibits dominant superconducting pairing correlations, with a sign difference between the bands. This is usually referred to as the d-wave -like superconducting phase of the two-leg ladder.<sup>11,27</sup>

The phase diagram in Fig. 6 confirms the results obtained along the line  $\Delta\mu = 0$ .<sup>11,27</sup> But it also indicates a limited stability of the various phases found at  $\Delta\mu = 0$  under inhomogeneously doping of the ladder. Upon increasing  $\Delta\mu$ , superconductivity is gradually suppressed, with intermediate phases showing residual superconducting fluctuations. Consider for example the low doping region where inter-band d-wave superconductivity occurs for vanishing  $\Delta\mu$ . While for small  $\Delta\mu > 0$  d-wave superconductivity sustains, inter-band phase coherence is lost when  $\Delta\mu$  reaches a value of approximately  $1.5t'$ . For larger values of  $\Delta\mu$  intra-band superconductivity persists within the lower band (which predominately projects onto the lower leg of the ladder). In the upper band spin fluctuations have become gapless and SDW and CDW correlations dominate. Further increase of  $\Delta\mu$  results in the suppression of all superconducting correlations, giving rise to two-band LL behavior. In the weakly interacting limit the upper band is depleted for  $\Delta\mu/t > 3.5$ , and a single-band LL, residing mainly on the lower leg of the ladder, dominates the large- $\Delta\mu$  regime. This progressive reduction of superconducting pairing correlations is also observed in the finite-temperature phase diagram. In Fig. 7 we show results for  $t' = t$ , and  $\Delta\mu/t = 0.3$  in the  $(\delta, T)$ -plane. From the renormalization of the energy scale,  $E \sim te^{-\pi l}$ , the logarithmic length scale of Eq. (22) can be related to a temperature scale  $T = E = T_0 e^{-\pi l}$ . While the phases of the system for  $T \rightarrow 0$  are found in accordance with Fig. 6, the finite temperature phase diagram reveals a successive enhancement of superconducting pairing correlations with decreasing temperature. Consider again the behavior close to half filling. At high temperatures the system is dominated by LL behavior in both bands. Upon decreasing the temperature gapless superconducting correlations develop within the lower band. At even lower temperatures, a finite spin gap opens for the lower band, then finally phase coherent inter-band d-wave superconductivity emerges, along with the opening of the second spin gap. Thus in an intermediate temperature regime, well above the onset of d-wave superconductivity, a single spin gap persists in the lower band, which is related to the bonding band at small values of  $\Delta\mu$ . This partial spin gap formation might be interpreted as a phenomenon similar to the pseudogap phase in the HTCS materials.

## VI. DISCUSSION AND CONCLUSION

For many years two-leg ladder systems have been prominent model systems for discussing superconductiv-

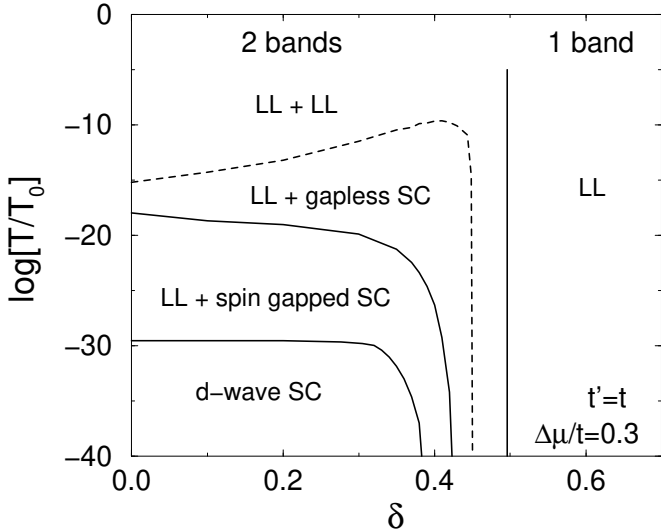


FIG. 7: Finite Temperature phase diagram of the inhomogeneously doped Hubbard model on the two-leg ladder in the weakly interacting limit for  $t' = t$ , and  $\Delta\mu/t = 0.3$ . Solid lines are phase boundaries, whereas the dashed line indicates a crossover inside the gapless regime.

ity in doped spin liquids. In this paper we investigated the stability of the superconducting phase, when doping occurs inhomogeneously. As anticipated from a strong coupling point of view a chemical potential difference between the legs of the ladder acts pair breaking, as could be clearly demonstrated in numerical exact diagonalization of finite systems.

Moreover, a mean field analysis based on the spinon-holon decomposition suggests that superconductivity is suppressed in steps. The imbalance of carrier distribution leads to a breakdown of the ordinary superconduct-

ing state of the ladder in favor of a superconducting state that resides mainly on the stronger doped leg. However, for this state the presence of the other leg is still important, since the tendency to pairing is associated with predominant dimer-singlet formation on the rungs. If the potential difference is sufficiently large, the holes fail to occupy the rungs in pairs and the pairing interaction is diminished. Eventually pairing does not occur anymore.

The same tendency is observed in the renormalization group treatment of the weakly interacting Hubbard model on the two-leg ladder. Inhomogeneous doping leads to a suppression of the superconducting phase, a Luther-Emery-liquid characterized by one gapless charge mode (C1S0). Moreover, an intermediate phase appears which corresponds to a single channel being superconducting while a coexisting channel forms a Luttinger liquid (C2S1). Analogous to the mean field result the extent of this phase increases towards larger doping concentrations. In both the  $t$ - $J$  and the Hubbard model a phase of complete destruction of superconducting fluctuations appears for large enough differences in the chemical potential. Within the renormalization group approach this normal phase is characterized as a single Luttinger liquid state (C1S1). While this identifies the true low-energy properties of this regime, the change in the spinon spectrum discussed in Sec. III rather reflects a short-coming of the mean-field solution.

In conclusion we emphasize that inhomogeneous doping of the two-leg ladder is harmful for the formation of the superconducting state. Furthermore, it can be an interesting tool to access new phases for this type of electronic systems.

We acknowledge fruitful discussions with Stephan Haas, Masashige Matsumoto, and Igor Milat. This work has been financially supported by the Swiss National-fund.

<sup>1</sup> P.W. Anderson, *Science* **235**, 1196 (1987).

<sup>2</sup> M. Fisher, in *Topological aspects of low-dimensional systems, Les Houches LXIX*, edited by A. Comtet *et al.* (EDP Sciences, Les Ulis & Springer, Paris, 1998); cond-mat/9806164.

<sup>3</sup> For a review, see T. Timusk and B. Statt, *Rep. Prog. Phys.* **62**, 61 (1999).

<sup>4</sup> R. Coldea, D.A. Tennant, A.M. Tsvelik, and Z. Tyliczynski, *Phys. Rev. Lett.* **86**, 1335 (2001).

<sup>5</sup> M. Azuma, Z. Hiroi, M. Takano, K. Ishida, and Y. Kitaoka, *Phys. Rev. Lett.* **73**, 3463 (1994).

<sup>6</sup> E. Dagotto and T.M. Rice, *Science* **271**, 618 (1996) and references therein.

<sup>7</sup> E. Dagotto, J. Riera, and D.J. Scalapino, *Phys. Rev. B* **45**, 5744 (1992).

<sup>8</sup> T.M. Rice, S. Gopalan, and M. Sigrist, *Europhys. Lett.* **23**, 445 (1993).

<sup>9</sup> C.A. Hayward, D. Poilblanc, R.M. Noack, D.J. Scalapino, and W. Hanke, *Phys. Rev. Lett.* **75**, 926 (1995).

<sup>10</sup> M. Troyer, H. Tsunetsugu, and T.M. Rice, *Phys. Rev. B* **53**, 251 (1996).

<sup>11</sup> L. Balents and M. Fisher, *Phys. Rev. B* **53**, 12133 (1996).

<sup>12</sup> For a review, see E. Dagotto, *Rep. Prog. Phys.* **62**, 1525 (1999).

<sup>13</sup> M. Uehara, T. Nagata, J. Akimitsu, H. Takahashi, N. Mori, and K. Kinoshita, *J. Phys. Soc. Japan* **65**, 2764 (1996).

<sup>14</sup> J.H. Schön, Ch. Kloc, R.C. Haddon, and B. Batlogg, *Science* **288**, 656 (2000).

<sup>15</sup> J.H. Schön, M. Dorget, F.C. Beuran, X.Z. Xu, E. Arushanov, M. Laguës, and C. Deville Cavellin, *Science* **293**, 2430 (2001).

<sup>16</sup> C.H. Ahn, T. Tybell, L. Antognazza, K. Char, R.H. Hammond, M.R. Beasley, O. Fischer and J.-M. Triscone, *Science* **276**, 1100 (1997).

<sup>17</sup> C.H. Ahn, S. Gariglio, P. Paruch, T. Tybell, L. Antognazza and J.-M. Triscone, *Science* **284**, 1152 (1999).

<sup>18</sup> S. Gariglio, C.H. Ahn, D. Matthey and J.-M. Triscone, *Phys. Rev. Lett.* **88**, 067002 (2002).

<sup>19</sup> Z. Hiroi and M. Takano, *Nature* **377**, 41 (1995).

<sup>20</sup> M. Sigrist, T.M. Rice, and F.-C. Zhang, *Phys. Rev. B* **49**, 12 058 (1993).

<sup>21</sup> C. Lanczos, *J. Res. Natl. Bur. Stand.* **45**, 255 (1950).

<sup>22</sup> The system with  $L=9$  also exhibits a clear tendency towards unbinding, however no level crossing but rather a crossover between the two regimes occurs. For  $L = 11$  a level crossing is found, with the total momentum jumping from 0 to a finite value near 0, whereas in the even systems the total momentum changes from 0 to a value near  $\pi$ . In view of these odd-even effect, we restrict the discussion to finite ladders with an even number of rungs.

<sup>23</sup> M.U. Ubbens and P. A. Lee, *Phys. Rev. B* **46**, 8434 (1992).

<sup>24</sup> T.M. Rice, S. Haas, M. Sigrist, and F.-C. Zhang, *Phys. Rev. B* **56**, 14 655 (1997).

<sup>25</sup> K. Le Hur, *Phys. Rev. B* **64**, R60502 (2001).

<sup>26</sup> V. J. Emery, S. A. Kivelson, and O. Zachar, *Phys. Rev. B* **56**, 6120 (1997).

<sup>27</sup> H. Lin, L. Balents, and M. Fisher, *Phys. Rev. B* **56**, 6569 (1997).

<sup>28</sup> H. Lin, L. Balents, and M. Fisher, *Phys. Rev. B* **58**, 1794 (1998).

<sup>29</sup> U. Ledermann, K. Le Hur, and T. M. Rice, *Phys. Rev. B* **62**, 16383 (2000).

<sup>30</sup> F.D.M. Haldane, *J. Phys. C* **14**, 2585 (1981).

<sup>31</sup> H.J. Schulz, in *Proceedings of Les Houches Summer School LXI*, edited by E. Akkermans *et al.* (Elsevier, Amsterdam, 1995).